Description of Scattering Object

A homogeneous low-loss dielectric almond proportional to the dimensions in [1].

Length Scale and Frequency Range

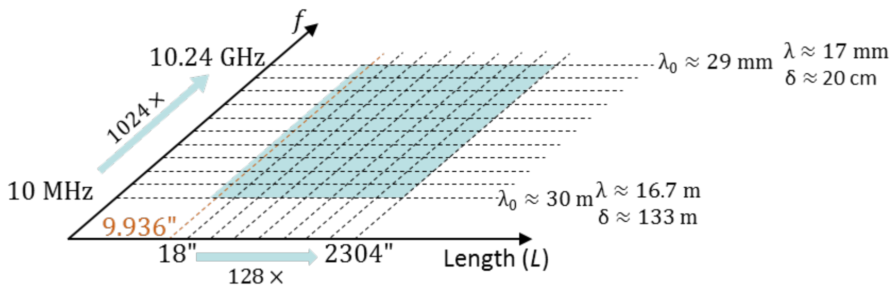

The problems of interest cover a range of ~256x in physical length scale and 1024x in frequency; the ranges are logarithmically sampled to yield 99 scattering problems. In these problems, the almond sizes are in the range $0.0076 \leq L/\lambda_0 \leq 1998$ and $1.7 \times 10^{-3} \leq L/\delta \leq 290$, where λ_0 is the free-space wavelength and δ is the penetration depth in the resin.

Interesting Features

1. The logarithmic sampling is distorted along the length axis for the smallest almond: the smallest almond has *L*=9.936'' (instead of *L*=9 in) because of publicly available measurement data corresponding to this size [1]-[3]. The sampling is also distorted along the frequency axis for the smallest almond: scattering from at frequencies $f \in$ {10, 20, 40, 80, 160, 320, 640, 1280, 2580, 5125, 7000, 10250} MHz are included in the problem set because of publicly available measurement data [3]. These distortions add 12 unique scattering problems to the set.
2. The non-trivial shape and tip of the almond presents modeling and meshing challenges.
3. The low-loss dielectric material introduces extra uncertainties and sensitivities to RCS measurements and simulations [3].

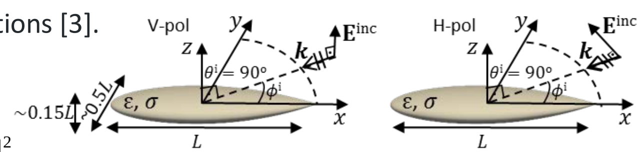

Quantities of Interest

Radar cross section (RCS) definition

$$\sigma_{vu}\left(\theta^{s},\phi^{s},\theta^{i},\phi^{i}\right)=\lim_{R\to\infty}4\pi R^{2}\frac{\left|\hat{v}\left(\theta^{s},\phi^{s}\right)\bullet\mathbf{E}^{\mathrm{scat}}\left(\theta^{s},\phi^{s}\right)\right|^{2}}{\left|\hat{u}\left(\theta^{i},\phi^{i}\right)\bullet\mathbf{E}^{\mathrm{inc}}\left(\theta^{i},\phi^{i}\right)\right|^{2}} \quad : \text{RCS } (\mathrm{m}^2)$$

$$\sigma_{vu,\mathrm{dB}}\left(\theta^{s},\phi^{s},\theta^{i},\phi^{i}\right)=10\log_{10}\sigma_{vu} \quad : \text{RCS in dB (dBsm)}$$

$$\sigma_{vu,\mathrm{dB}}^{TH}\left(\theta^{s},\phi^{s},\theta^{i},\phi^{i}\right)=\max(\sigma_{vu,\mathrm{dB}},TH_{vu,\mathrm{dB}})-TH_{vu,\mathrm{dB}} \quad : \text{Thresholded RCS}$$

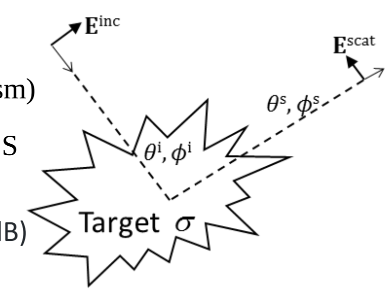

1. Set $\theta^{\mathrm{i}} = 90^{\mathrm{o}}$. Vary $0^{\mathrm{o}} \leq \phi^{\mathrm{i}} \leq 180^{\mathrm{o}}$ (every 0.5^{o} in the interval).
2. Compute back-scattered $\sigma_{\theta\theta,\mathrm{dB}}$ and $\sigma_{\phi\phi,\mathrm{dB}}$ (the VV- and HH-RCS in dB) at $N_{\phi} = 361$ scattering directions.

Material Properties

The permeability of the resin is the same as that of free space. A Debye model expressed as $\epsilon(f) = \epsilon_0\varepsilon_r(f)$, where

$$\varepsilon_r(f) = \varepsilon_r'(f) - j\varepsilon_r''(f) = 2.85 - j0.0687 + \frac{0.365 - j0.0602}{1 - jf(-0.1135 + j0.899)}$$

was used to calculate the complex permittivity of resin at the frequencies of interest. The reference simulation results were computed using precisely the permittivity values (i.e., to machine precision) shown in the below table. The above Debye model for the resin is slightly different than that in [3]. This is because a second set of measurements were performed following the submission of [3] that yielded slightly different values for the dielectric properties [4]. The average of the two measurements are used to fit the above Debye model as described in [4].

Frequency f (MHz)	ϵ'	ϵ''	Frequency f (MHz)	ϵ'	ϵ''
10	3.21	1.29×10^{-1}	2560	2.96	9.64×10^{-2}
20	3.21	1.29×10^{-1}	2580	2.96	9.63×10^{-2}
40	3.20	1.28×10^{-1}	5120	2.91	8.60×10^{-2}
80	3.19	1.28×10^{-1}	5125	2.91	8.60×10^{-2}
160	3.17	1.26×10^{-1}	7000	2.90	8.22×10^{-2}
320	3.13	1.23×10^{-1}	10 240	2.88	7.85×10^{-2}
640	3.08	1.18×10^{-1}	10 250	2.88	7.85×10^{-2}
1280	3.02	1.08×10^{-1}			

Performance Measures

Error Measure: Simulation errors shall be quantified using

$$avg.err_{uu,\mathrm{dB}}^{TH} = \frac{1}{2\pi}\int_0^{2\pi}\left|\sigma_{uu,\mathrm{dB}}^{TH}\left(\phi^s\right) - \sigma_{uu,\mathrm{dB}}^{\mathrm{ref},TH}\left(\phi^s\right)\right| d\phi^s \approx \frac{1}{N_\phi}\sum_{n=1}^{N_\phi}\left|\sigma_{uu,\mathrm{dB}}^{TH}\left(\phi^s\right) - \sigma_{uu,\mathrm{dB}}^{\mathrm{ref},TH}\left(\phi^s\right)\right| \ (\mathrm{dB}) \ \text{ for } u \in \{\theta, \phi\}$$

where

$$TH_{uu,\mathrm{dB}} = \max_{\phi^s} \sigma_{uu,\mathrm{dB}}^{\mathrm{ref}} - 80 \ (\mathrm{dB})$$

This error measure discounts errors in RCS values below TH .

Cost Measure: Simulation costs shall be quantified using observed wall-clock time and peak memory/core

$$t_{\mathrm{main}}^{\mathrm{wall}} \text{ (s) and } mem_{\mathrm{main}}^{\mathrm{maxcore}} \text{ (bytes)}$$

as well as the “serialized” CPU time and total memory requirement

$$t_{\mathrm{main}}^{\mathrm{total}} = N_{\mathrm{proc}} \times t_{\mathrm{main}}^{\mathrm{wall}} \text{ (s) and } mem_{\mathrm{main}}^{\mathrm{max}} = N_{\mathrm{proc}} \times mem_{\mathrm{main}}^{\mathrm{maxcore}} \text{ (bytes)}$$

Here, N_{proc} denotes the number of processes used in a parallel simulation. It is expected that results will be reported for at least 2 runs: “Efficient” (small N_{proc}) and “Fast” (large N_{proc}).

Study 1: Error vs. Cost Sweep

Fix frequency and fix almond dimensions. Simulate many error levels (proxy: mesh densities) for 4 cases:

Case 1: *f*=10 MHz, *L*=9.936 in
Case 2: *f*=7 GHz, *L*=9.936 in
Case 3: *f*=10 MHz, *L*=288 in
Case 4: *f*=320 MHz, *L*=288 in

It’s recommended to simulate as many error levels (mesh densities) as possible. 3-5 error levels is typical. A typical error-vs.-cost study will consist of 4x3-5=12-20 simulations.

Study 2: Frequency Sweep

Fix almond dimensions and error level (proxy: mesh density). Simulate many frequencies for 4 cases:

Case 1: *L*=18 in, error level 1 (coarsest mesh)
Case 2: *L*=288 in, error level 1 (coarsest mesh)
Case 3: *L*=18 in, error level 2 (finer mesh)
Case 4: *L*=288 in, error level 2 (finer mesh)

Frequencies shall be chosen as $f \in \{10, 20, 40, \dots, 5120, 10240\}$ MHz. It’s recommended to simulate as many frequencies as possible. A full frequency-sweep study will consist of 4x11=44 simulations.

Study 3: Size Sweep

Fix frequency and error level (proxy: mesh density). Simulate many sizes for 4 cases:

Case 1: *f*=10 MHz, error level 1 (coarsest mesh)
Case 2: *f*=320 MHz, error level 1 (coarsest mesh)
Case 3: *f*=10 MHz, error level 2 (finer mesh)
Case 4: *f*=320 MHz, error level 2 (finer mesh)

Dimensions shall be chosen as $L \in \{9.936, 18, 36, \dots, 1152, 2304\}$ in. It’s recommended to simulate as many sizes as possible. A full size-sweep study will consist of 4x9=36 simulations.

Reference Quantities of Interest

The following RCS data are made available in the benchmark to enable participants to calibrate their simulators:

4 RCS measurement results corresponding to the smallest almond (*L*=9.936 in) at frequencies $f \in$ {2580, 5125, 7000, 10250} MHz. These measurements were made using an almond of size *L*=9.936 in. These data are the same as those plotted in Fig. 13 of [3]; they are provided for ϕ^{i} sampled every 0.5^{o}.

4 RCS simulation results for the smallest almond at the above 4 frequencies found by using the ARCHIE-AIM code, a frequency-domain FFT-accelerated integral-equation solver developed at UT Austin [5]-[7]. These data are obtained using the finest mesh (≈0.6-mm average edge length) shown in [2].

References

[1] A. C. Woo, H. T. G. Wang, M. J. Schuh and M. L. Sanders, "EM programmer's notebook-benchmark radar targets for the validation of computational electromagnetics programs," *IEEE Ant. Propag. Soc. Mag.*, vol. 35, no. 1, pp. 84-89, Feb. 1993.

[2] J. T. Kelley, D. A. Chamulak, C. C. Courtney, and A. E. Yilmaz, "Rye Canyon radar cross-section measurements of benchmark almond targets," *IEEE Ant. Popag. Soc. Mag.*, Feb. 2020.

[3] J. T. Kelley, A. E. Yilmaz, D. A. Chamulak, and C. C. Courtney, "Measurements of non-metallic targets for the Austin RCS benchmark suite," in *Proc. Ant. Meas. Tech. Assoc. (AMTA) Symp.*, Oct. 2019.

[4] J. T. Kelley, D. A. Chamulak, C. C. Courtney, and A. E. Yilmaz, "Measurements of non-metallic targets for the Austin RCS benchmark suite," *presentation in AMTA Symp.,* Oct. 2019. Available: https://github.com/UTAustinCEMGroup/AustinCEMBenchmarks/Austin-RCS-Benchmarks/AMTA2019presentation.pdf

[5] M. F. Wu, G. Kaur, and A. E. Yılmaz, "A multiple-grid adaptive integral method for multi-region problems," *IEEE Trans. Antennas Propag.*, vol. 58, no. 5, pp. 1601-1613, May 2010.

[6] F. Wei and A. E. Yılmaz, "A more scalable and efficient parallelization of the adaptive integral method part I: algorithm," *IEEE Trans. Antennas Propag.*, vol. 62, no.2, pp. 714-726, Feb. 2014.

[7] J. W. Massey, V. Subramanian, C. Liu, and A. E. Yılmaz, "Analyzing UHF band antennas near humans with a fast integral-equation method," in *Proc. EUCAP*, Apr. 2016.